

cyanquinodimethane.

We are grateful to L. V. Interrante for useful discussions.

¹*Extended Interactions between Metal Ions*, edited by L. V. Interrante, American Chemical Society Symposium Series No. 5 (American Chemical Society, Washington, D. C., 1974).

²*Low-Dimensional Cooperative Phenomena*, edited by H. J. Keller (Plenum, New York, 1975).

³H. R. Zeller, *Adv. Solid State Phys.* **13**, 31 (1973).

⁴M. J. Rice and S. Strässler, *Solid State Commun.* **13**, 125 (1973).

⁵M. J. Rice, in Ref. 2, p. 23.

⁶A. N. Bloch and R. B. Weisman, in Ref. 1, p. 356.

⁷B. Renker, H. Rietschel, L. Pintschovius, W. Gläser, P. Brüesch, D. Kuse, and M. J. Rice, *Phys. Rev. Lett.* **30**, 1144 (1973).

⁸R. Combès, M. Lambert, H. Launois, and H. R. Zeller, *Phys. Rev. B* **8**, 571 (1973).

⁹H. R. Zeller, in Ref. 2, p. 215.

¹⁰H. R. Zeller and P. Brüesch, *Phys. Status Solidi (b)* **65**, 537 (1974).

¹¹R. Hoffman, *J. Chem. Phys.* **39**, 1397 (1963).

¹²R. P. Messmer, *Chem. Phys. Lett.* **11**, 589 (1971).

¹³L. V. Interrante and R. P. Messmer, *Inorg. Chem.* **10**, 1174 (1971).

¹⁴D. M. Whitmore, Ph. D. thesis, Stanford University, 1974 (unpublished).

¹⁵L. V. Interrante and R. P. Messmer; in Ref. 1, p. 382.

Effect of the Surface Energy of Electron-Hole Drops on Their Luminescence Spectrum in Ge

B. Etienne,* C. Benoît à la Guillaume, and M. Voos

Groupe de Physique des Solides† de l'École Normale Supérieure, Université Paris VII, 75005 Paris, France

(Received 15 May 1975)

The size of small electron-hole drops near threshold is investigated in Ge using a small shift of their main luminescence line due to their surface energy σ . The smallest radii measured at different temperatures are compared with the minimum stable radii given by a model taking σ and the drop binding energy φ into account. We find an excellent agreement if we use the spectroscopic value of φ (23 K).

Experimental and theoretical investigations of electron-hole drops (EHD's) in Ge have received much attention during the last five years. Most of the work to date has been devoted to measuring and understanding bulk properties of this liquid phase.¹ However, different authors² have calculated recently the EHD surface energy σ which is $\sigma \sim 10^{-4}$ erg/cm² in Ge. This quantity has been also estimated from light-scattering measurements by Alekseev *et al.*³ ($\sigma = 1.6 \times 10^{-4}$ erg/cm²) and by Silver⁴ ($\sigma = 10^{-3}$ erg/cm²).

We report here experiments showing that for small EHD's their surface energy has an effect on their luminescence. Indeed, using a sensitive differential method, we have observed that the LA-phonon-assisted emission line of EHD's in Ge shifts towards high energy with decreasing excitation level (J) when it is not too far from the threshold J_{th} for EHD formation. This is explained by a change in the EHD chemical potential due to σ and provides a determination of the mean EHD radius. The temperature dependence of the smallest measured radii is in very good agreement with that of the minimum stable radii given by a

simple model which takes σ into account. This model allows us to get from our data the ratio A/σ , where A is the Richardson-Dushman constant. The agreement with the theoretical value of A/σ is satisfying if we use the spectroscopic value⁵ of the EHD binding energy (23 K).

The idea of the experiments reported here is to measure near J_{th} the shift ΔE in the luminescence line of the EHD's when their size changes. As shown below, the size of EHD's depends on the pump level and also, because of hysteresis,⁶ on the pump-level history. In these experiments, a pure Ge sample ($N_A - N_D \sim 2 \times 10^{10}$ cm⁻³) is immersed in liquid He and excited by a stable cw mercury or halogen lamp monitored with a special chopper as shown in Figs. 1(a) and 1(b), so that both levels of excitation J_1 and J_2 , whose ratio was always equal to 10, have opposite phases. The corresponding luminescence lines, which are analyzed with a grating spectrometer followed by a PbS cell, are sent into a lock-in amplifier and are normalized by adjusting the duration of J_1 so that they have the same amplitude at their maximum. The resulting signal is thus pro-

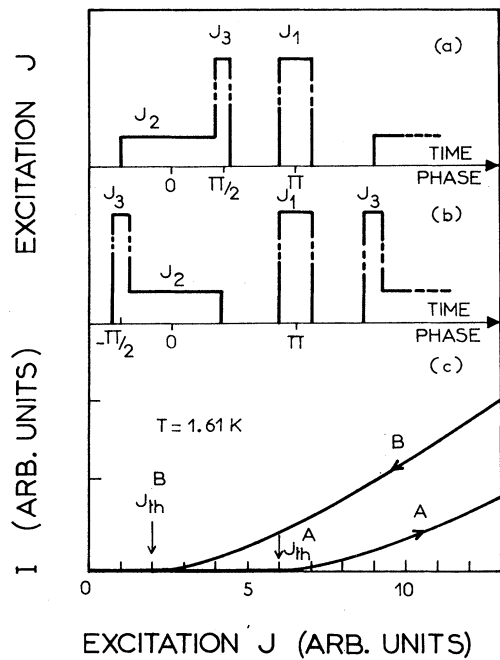


FIG. 1. (a), (b) Schematized time and phase dependence of the excitation. The chopping frequency is 75 Hz. (c) Luminescence signal I of the 709-meV EHD line versus excitation J , as J is continuously increased from zero to 1000 (off scale) and back to zero ($J_{th}^B \sim 20 \mu\text{W}/\text{mm}^2$).

portional to the difference between these lines and the change in the luminescence spectra corresponding to J_1 and J_2 is greatly amplified. Besides, putting just before J_2 [Fig. 1(b)] an excitation J_3 equal to J_1 and in phase quadrature with J_1 and J_2 allows measurements on the descending branch (curve B) of the optical hysteresis⁶ shown in Fig. 1(c). The excitation scheme represented in Fig. 1(a) gives data on the rising branch (curve A); here J_3 is not functional but is left for convenience.

Typical data obtained on branch B at 1.6 K are shown in Fig. 2(a) for $J_2 \sim 10J_{th}^B$. The peaks at 713.6 and 705.2 meV are due to the well-known LA and TO phonon replicas of free excitons. At the position of the LA phonon-assisted emission line of EHD's (~ 709 meV), one can see a positive and a negative bump which reveal a shift (ΔE) of this line towards high energy for the lower excitation (J_2) with respect to its position relative to the larger one (J_1). This shift decreases when the excitation is increased and for $J_2 \gg J_{th}^B$ no effect could be detected.

To explain our results we consider an EHD consisting of N electron-hole pairs in a volume V

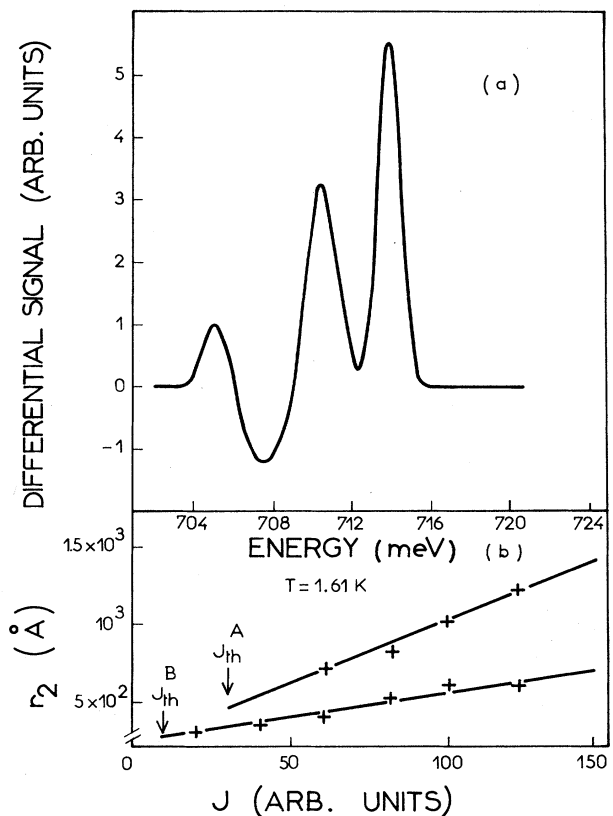


FIG. 2. (a) Typical differential luminescence signal at 1.61 K for $J_2 \sim 10J_{th}^B$. ΔE is obtained from the intensities of the positive bump and of the normal (i.e., not differentiated) signal at 709 meV which is here 8 times larger than the 714-meV peak shown in this figure. (b) Variation with excitation of r_2 on branches A and B of the hysteresis shown in Fig. 1(c).

$= 4\pi r^3/3$. At $T=0$, its total energy is $E = NE_G + 4\pi r^2\sigma$, where E_G is the EHD ground-state energy per electron-hole pair calculated in the case of an infinite EHD. The chemical potential of an EHD of radius r is given by $\mu(r) = \partial E/\partial N = \mu(\infty) + 2\sigma/n_0 r$, where⁷ $\mu(\infty) = E_G$ and n_0 is the density of electron-hole pairs in an infinite drop.⁸ Since the EHD chemical potential is obtained from the high-energy cutoff of the 709-meV line, for instance, it is clear that in the case of a small EHD this line should shift towards high energy with respect to the recombination peak, corresponding to a large EHD.⁹ We believe that this model is applicable to our results with $\Delta E = (1/r_2 - 1/r_1)2\sigma/n_0$, where r_1 and r_2 are the mean radii corresponding respectively to J_1 and J_2 . We neglect $2\sigma/r_1 n_0$ because, as can be deduced from Fig. 2(b), the resulting error on the determination of r_2 is equal to $\sim 20\%$ and is comparable to

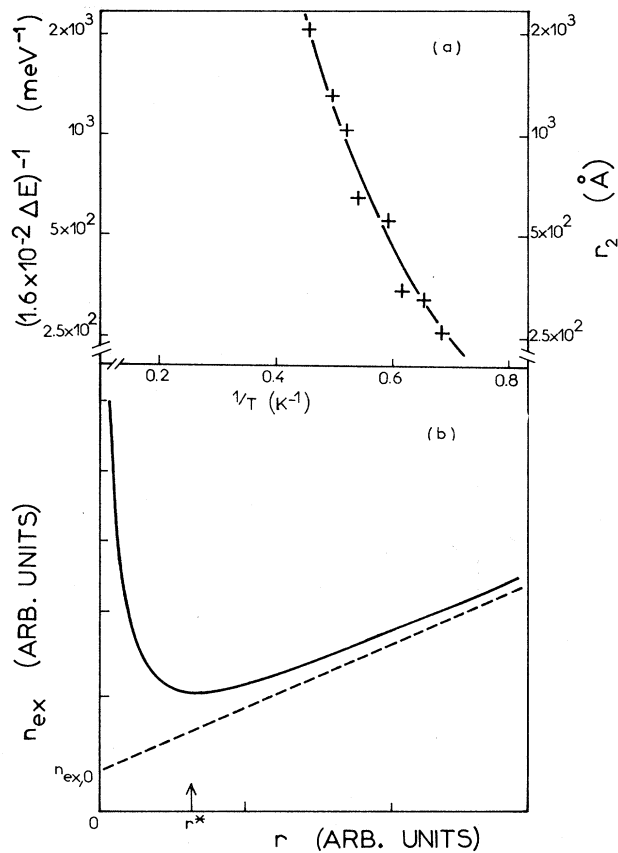


FIG. 3. (a) Experimental temperature dependence (pluses) of ΔE for $J_2 \sim 2J_{th}^B$. The corresponding values of r_2 were obtained with $\sigma = 10^{-4}$ erg/cm². The solid line is a fit to the experimental values of ΔE with $\varphi(\infty) = 23$ K and $A/\sigma = 1.6 \times 10^{14}$ sec⁻¹ K⁻² erg⁻¹ cm². (b) n_{ex} as a function of r in the model of Pokrovskii (dashed line). The solid line represents the general behavior of n_{ex} versus r when the EHD surface energy is taken into account.

the experimental accuracy. Using the theoretical value of σ , one can obtain the curves given in Figs. 2(b) and 3(a). Figure 2(b) gives the variation of r_2 versus excitation on the branches A and B shown in Fig. 1(c). Figure 3(a) represents the observed temperature dependence of the values of ΔE and r_2 obtained on branch B for an excitation J_2 as close to J_{th}^B as possible.

Now, considering the previous model, it is obvious that the EHD work function φ is $\varphi(r) = \varphi(\infty) - 2\sigma/rm_0$. Therefore the well-known Pokrovskii equation¹ giving the mean density n_{ex} of the exciton gas as a function of r should be modified; it then becomes⁴ $n_{ex} = \alpha r + n_{ex,0} \exp(2\sigma/rm_0 kT)$. Here $\alpha = 4n_0/3v_{ex}\tau_0$, where v_{ex} is the exciton thermal

velocity and τ_0 is the EHD lifetime; $n_{ex,0} = g(2\pi m^* \times kT/h^2)^{3/2} \exp[-\varphi(\infty)/kT]$, where g and m^* are respectively the exciton degeneracy and mass. The general behavior of n_{ex} versus r is shown in Fig. 3(b). Clearly only radii larger than r^* are stable⁴ and r^* is the smallest stable radius which is given by

$$r^* = \beta(A\sigma T)^{1/2} \exp[-\varphi(\infty)/kT] \times \exp(\sigma/r^*n_0kT), \quad (1)$$

where

$$\beta^2 = 2\tau_0 \left(\frac{3}{4}\pi\right)^{1/3} / kn_0^{4/3}$$

and

$$A = (3\pi^2/4n_0)^{2/3} 8m^* g k^2/h^3$$

with¹ $n_0 = 2 \times 10^{17}$ cm⁻³ and $\tau_0 = 40$ μ sec.

When the excitation is increased from zero, some supersaturation is needed to create EHD's so that J_{th}^A and branch A of Fig. 1(c) correspond to $r > r^*$. On the contrary, when the excitation is reduced from some value greater than J_{th}^A , the radius of the EHD's can decrease down to r^* at the threshold J_{th}^B . Therefore, as can be deduced from Fig. 2(b), the experimental values of ΔE given in Fig. 3(a) can be taken equal to $2\sigma/r^*n_0$. Putting $r^* = 2\sigma/n_0\Delta E$ in Eq. (1) yields

$$\frac{1}{\Delta E} \exp\left(\frac{-\Delta E}{2kT}\right) = \frac{\beta n_0}{2} \left(\frac{AT}{\sigma}\right)^{1/2} \exp\left[\frac{-\varphi(\infty)}{kT}\right]. \quad (2)$$

This expression depends on $\varphi(\infty)$ and A/σ and, taking $\varphi(\infty) = 23$ K, an excellent fit to the experimental data $\Delta E(T)$ is obtained for $A/\sigma \sim 1.6 \times 10^{14}$ sec⁻¹ K⁻² erg⁻¹ cm², as shown in Fig. 3(a). Using the theoretical values of σ and A (3.2×10^{10} sec⁻¹ K⁻²), A being calculated with the most often quoted values of m^* ($0.33m_0$) and g (16), we get $(A/\sigma)_{th} = 3.2 \times 10^{14}$ sec⁻¹ K⁻² erg⁻¹ cm², in good agreement with experiment. On the other hand, using $\varphi(\infty) = 16$ K, we can fit our data with $A/\sigma = (A/\sigma)_{th}/120$, which is not reasonable though A and σ are not very well known. Therefore, considering our results, it is believed that $\varphi(\infty)$ is closer to 23 K than to 16 K. It is thought that the experimental data used^{6,10} to get $\varphi = 16$ K should be reanalyzed because, as will be shown in a forthcoming paper, supersaturation effects should be taken into account to interpret these data.

One of us (M.V.) would like to thank J. M. Worlock for useful discussions.

*Work supported by a Direction des Recherches et Mogens d'Essais, Ministère des Armées, fellowship.

†Laboratoire associé au Centre National de la Recherche Scientifique.

¹See, for example, Y. A. Pokrovskii, *Phys. Status Solidi (a)* **11**, 385 (1972); T. M. Rice, in *Proceedings of the Twelfth International Conference on the Physics of Semiconductors, Stuttgart, Germany, 1974*, edited by M. H. Pilkuhn (Teubner, Stuttgart, Germany, 1974), p. 23; M. Voos, *ibid.*, p. 33, and references therein.

²L. M. Sander, H. B. Shore, and L. J. Sham, *Phys. Rev. Lett.* **31**, 533 (1973); H. Buttner and E. Gerlach, *J. Phys. E: Sci. Instrum.* **6**, L433 (1973); T. M. Rice, *Phys. Rev. B* **9**, 1540 (1974); T. L. Reinecke and S. C. Ying, *Solid State Commun.* **14**, 381 (1974).

³A. S. Alekseev, T. A. Astemirov, V. S. Bagaev, T. I. Galkina, N. A. Penin, N. N. Sybeldin, and V. A. Tsvetkov, in *Proceedings of the Twelfth International Conference on the Physics of Semiconductors, Stuttgart, Germany, 1974*, edited by M. H. Pilkuhn (Teubner, Stuttgart, Germany, 1974), p. 91.

⁴R. N. Silver, *Phys. Rev. B* **11**, 1569 (1975).

⁵C. Benoît à la Guillaume and M. Voos, *Solid State Commun.* **12**, 1257 (1973); G. A. Thomas, T. G. Phillips, T. M. Rice, and J. C. Hensel, *Phys. Rev. Lett.*

31, 386 (1973); T. K. Lo, *Solid State Commun.* **15**, 1231 (1974).

⁶T. K. Lo, B. J. Feldman, and C. D. Jeffries, *Phys. Rev. Lett.* **31**, 224 (1973).

⁷See, for example, W. F. Brinkman and T. M. Rice, *Phys. Rev. B* **7**, 1508 (1973).

⁸It can be shown that an increase of n_0 can diminish the total energy of an EHD if σ is considered. This change is proportional to $1/r$ and gives a $1/r^2$ contribution which is negligible with respect to the $2\sigma/n_0r$ correction.

⁹The differential spectrum of the 709-meV line should then look exactly like the derivative of the normal emission line, and the areas of the corresponding positive and negative bumps shown in Fig. 2(a) should be equal. Even if we take into account the contribution of the 705-meV line, there is still a small difference between these areas which can be explained by a change in the bulk density.

¹⁰J. C. Hensel, T. G. Phillips, and T. M. Rice, *Phys. Rev. Lett.* **30**, 227 (1973); J. C. McGroddy, M. Voos, and O. Christensen, *Solid State Commun.* **13**, 1801 (1973); Pokrovskii, Ref. 1.

Composition and Energy Spectra of Heavy Nuclei of Unknown Origin Detected on Skylab*

J. H. Chan and P. B. Price

Department of Physics, University of California, Berkeley, California 94720

(Received 24 March 1975)

At the orbit of Skylab we observed steeply falling energy spectra of nuclei with $Z \geq 8$ and $10 \lesssim E \lesssim 40$ MeV/amu at intensities much higher than seen outside the magnetosphere. The composition is O:Ne:[Na-Si]:Fe = 100:33:13:(~2), consistent with that of the solar corona. We suggest that heavy solar-wind ions enter the magnetosphere, are accelerated, and populate the inner radiation belt.

Lexan track detectors with large collecting power were exposed both outside and inside the Skylab during late 1973 and early 1974. The earth's field excludes from direct access to the Skylab orbit (inclination 52° , altitude 420 km) most particles of energy less than a few hundred MeV/amu that originate outside the magnetosphere. We were therefore surprised to discover a high density of tracks of nuclei with $Z \geq 8$ in the Lexan, indicating a novel source of charged particles with a steep energy spectrum and roughly solar composition, at the orbit of Skylab.

The external detector consisted of a 180-cm² stack of 32 sheets of Lexan, total thickness 1 g/cm², wrapped in thin aluminum tape, and clamped to part of the Apollo telescope mount with its plane parallel to the sun direction, so as to minimize heating. Both sides were exposed to

space from 22 November 1973 to 3 February 1974. To study particles with energy greater than ~ 100 MeV/amu, we examined one of 35 Lexan stacks exposed from 29 May 1973 to 5 February 1974 inside the Skylab (primarily intended for the study of ultraheavy cosmic rays).

Lexan exposed to the ultrahigh vacuum of space has a weaker response to charged particles than does Lexan exposed in a partial pressure of oxygen. To amplify this weak response, we processed the Lexan in four stages, first by a short irradiation with uv light of $\sim 3100 \text{ \AA}$, then by an etch in 6.25N NaOH at 40°C , then by a long irradiation with the same uv light, then by an additional etch in NaOH. Each resulting etch pit has a "shoulder" that permitted both ionization rate and total range to be inferred from its shape and dimensions.¹